EUROPEAN FUSION DEVELOPMENT AGREEMENT

EFDA–JET–PR(04)68

J. Stober, P.J. Lomas, G. Saibene, Y. Andrew, P. Belo, G.D. Conway,
A. Herrmann, L.D. Horton, M. Kempenaars, H-R. Koslowski, A. Loarte,
G.P. Maddison, M. Maraschek, D.C. McDonald, A.G. Meigs,
P. Monier-Garbet, D.A. Mossessian, M.F.F. Nave, N. Oyama, V. Parail,
Ch P. Perez, F. Rimini, R. Sartori, A.C.C. Sips, P.R. Thomas,
the ASDEX Upgrade Team and EFDA JET contributors

Small ELM Regimes with good Confinement on JET and Comparison to those on ASDEX Upgrade, Alcator C-mod, and JT-60U

Small ELM Regimes with good Confinement on JET and Comparison to those on ASDEX Upgrade, Alcator C-mod, and JT-60U

J. Stober[1], P.J. Lomas[2], G. Saibene[3], Y. Andrew[2], P. Belo[4], G.D. Conway[1], A. Herrmann[1], L.D. Horton[1], M. Kempenaars[5], H-R. Koslowski[6], A. Loarte[3], G.P. Maddison[2], M. Maraschek[1], D.C. McDonald[2], A.G. Meigs[2], P. Monier-Garbet[7], D.A. Mossessian[8], M.F.F. Nave[4], N. Oyama[9], V. Parail[2], Ch P. Perez[6], F. Rimini[7], R. Sartori[3], A.C.C. Sips[1], P.R. Thomas[7], the ASDEX Upgrade Team and EFDA JET contributors*

[1]MPI für Plasmaphysik, EURATOM Association, D-85748 Garching, GERMANY
[2]Euratom/UKAEA Association, Culham Science Centre, Abingdon, OX14 3DB, UK
[3]EFDA Close Support Unit (Garching), 2 Boltzmannstrasse, Garching, Germany
[4]Associação EURATOM/IST, Centro de Fusòao Nuclear, 1049-001 Lisbon, Portugal
[5]FOM-Rijnhuizen, Association Euratom-FOM, TEC, PO Box 1207, Nieuwegein, The Netherlands
[6]Forschungszentrum Jülich GmbH, Institut fur Plasmaphysik, EURATOM Association, Trilateral Euregio Cluster, 52425 Jülich, Germany
[7]Association Euratom-CEA, Cadarache, F-13108 St. Paul-lez-Durance, France
[8]Massachusetts Institute of Technology Cambridge, MA, USA
[9]JAERI, Naka Fusion Research Establishment, Naka-machi, Naka-gun, Ibaraki-ken, 311-01, Japan
See appendix of J. Pamela et al., "Overview of JET results", in Proc of 19th IAEA Fusion EnergyConference, Lyon, 2002 (IAEA, Vienna, 2003) Partner in the Trilateral Euregio Cluster (TEC)*

Preprint of Paper to be submitted for publication in
Nuclear Fusion

ABSTRACT

Since it is uncertain if ITER operation is compatible with type-I ELMs, the study of alternative ELM regimes is an urgent issue. This paper reports on experiments on JET aiming to nd scenarios with small ELMs and good confinement, such as the type-II ELMs in ASDEX Upgrade, the enhanced D-alpha H-mode in Alcator C-mod or the grassy ELMs in JT-60U. The study includes shape variations, especially the closeness to a double-null configuration, variations of q_{95}, density and beta poloidal. H-mode pedestals without type-I ELMs have been observed only at the lowest currents ($\leq$ 1.2MA), showing similarities to the observations in the devices mentioned above. These are discussed in detail on the basis of edge fluctuation analysis. For higher currents, only the mixed type-I/II scenario is observed. Although the increased inter-ELM transport reduces the type-I ELM frequency, a single type-I ELM is not significantly reduced in size. Obviously, these results do question the accessibility of such small ELM scenarios on ITER, except perhaps the high beta-poloidal scenario at higher q_{95}, which could not be tested at higher currents at JET due to limitations in heating power.

1. INTRODUCTION

Estimates of the amplitude of Edge Localized Modes (ELMs) for the planed international test reactor ITER indicate that the peak power flux due to the expected type-I ELMs could severely limit the divertor lifetime for the standard Q=10 (i.e. $P_{fus} = 10 \times P_{in}$) scenario at $q_{95} = 3$. The divertor lifetime could be as low as a few hundred discharges, although this depends strongly on the physics assumptions [1]. To be prepared for the worst case, techniques for ELM mitigation/control are being developed. This contribution reports on efforts to establish in the world's largest operational tokamak JET regimes with smaller (or no) ELMs and sufficient particle exhaust but nevertheless good H-mode energy confinement. The latter means that the ratio of the experimental energy confinement time τ_E to the scaled energy confinement time $\tau_{E,\,scal}$ according to the actual ITER scaling IPB98(y,2) [2] should be close to unity. This ratio is usually refered to as H-factor H98(y,2). The experiments described in the following are based on strategies derived from successful experiments on other devices, i.e. type-II ELMs on ASDEX Upgrade [3,4], grassy ELMs on JT-60U[5,6], and the "Enhanced D-Alpha" (EDA) H-Mode on Alcator C-mod[7,8]. The Quiescent H-mode (QH) on DIII-D and ASDEX Upgrade has also been attempted in JET and is reported in a separate contribution [9].

As a starting point for these small ELM studies, the JET mixed type-I/II regime was chosen [10]. In these H-modes, increased edge transport in between type-I ELMs is observed in hightriangularity (high-δ) equilibria at high density (>80% of the Greenwald density n_{GW}), up to a plasma current of 3MA, the latter limitted only by the available additional heating power [11]. Due to some similarities in the divertor-D_α traces and due to the observed increase of magnetic activity and power-flux across the separatrix between ELMs these phases were called mixed type-I/II phases, in analogy to similar observations on other machines. Figure 1 illustrates the effect of the mixed

type-I/II ELMs on the power- flux across the separatrix due to ELMs and in between ELMs. The slopes in the left part of the figure indicate that for these two discharges with almost identical parameters, the inter-ELM transport in the mixed type-I/II phase is significantly higher than in the pure type-I phase (less transport leads to faster energy rise). The right part of the figure quantifies this for several phases and varying shape (as will be discussed in the next section). It shows that during these mixed type-I/II phases the inter-ELM power flux can double from 40% (as observed in pure type-I ELM phases at slightly lower density) to 80% of the time-averaged power crossing the separatrix. But a comparison of the drops in the stored energy due to type-I ELMs in the upper and lower curve of the left part of the figure also shows that the type-I ELMs in the mixed type-I/II phase which eject the remaining 20% of power are similar in size to those observed in the pure type-I ELM phases at slightly lower densities. For these conditions we find $\Delta W \approx$ 150-200kJ and $\Delta W/W \approx 3\%$. For a more detailed discussion of ELM sizes in mixed type-I/II ELMy phase see [12]. It was reported in [13] that the enhanced inter-ELM transport is related to an increase in strength of broadband MHD modes moving in the direction of the electron diamagnetic drift with frequencies between 10kHz and 40kHz, which are called at JET washboard-modes (WB) [14]. In the same frequency range one finds enhanced density fluctuations close to the pedestal top with the far-infrared-interferometer [12]. In contrast to the type-II ELMs of ASDEX Upgrade, no high-frequent irregular bursty events in the type-II phases in between type-I ELMs were found at JET[10, 13, 12]. Only recently, at the lowest plasma currents, i.e. I_p = 1.1MA, smaller bursts in between the bigger ones have been found in magnetic and edge-density signals (Fig.2). This indicates that the burstyness of the additional inter-ELM transport is not necessarily a good criterion to differentiate between small ELM types, but does itself depend on the actual pedestal parameters.

As explained above, the main drawback of the mixed type-I/II phase at JET are the remaining type-I ELMs, which still are a potential danger for the divertor of a future reactor. Therefore, additional efforts to further increase the inter-ELM transport on JET were undertaken and are described in the following sections. As these were stimulated by successful scenarios on other devices, this paper focuses on the inter-machine comparision of the results. Further detailed analysis of the JET results is found in [12, 15, 16]. Section 2 describes how the mixed I/II regime reacts to increasing edge safety factor q_{95} and the closeness to a double null configuration (DN), which have been identified as helpful on other devices. Section 3 describes the attempts to match in JET the EDA H-mode of Alcator C-mod and the type-II ELMy H-mode of ASDEX Upgrade with dimensionless identical plasmas to facilitate a scenario transfer. Section 4 reports on attempts to obtain the high β_{pol}-scheme on JET and ASDEX Upgrade, which is the basis for the grassy ELM operation in JT-60U.

2. EFFECT OF DN AND INCREASED Q_{95} ON THE JET MIXED TYPE-I/II ELM REGIME

The results of the ASDEX Upgrade type-II ELMs showed that a quasi-DN (QDN) configuration is an essential ingredient for that regime [3]. Therefore a SN(Single-Null)- configuration of JET which

shows the mixed type-I/II regime was modified to be close to DN and still compatible with operation at 2.5MA plasma current. The right part of Fig.1 shows that the contribution of inter-ELM losses in the mixed type-I/II phases is similar for the SN and QDN shapes. In fact the confinement was often decreasing by up to 10% when approaching QDN, but it cannot be excluded that this is due to insufficient conditioning of the upper divertor, which is only rarely used.

Both for SN and QDN configurations, q_{95} has been increased, following the experience from other devices, in which increased inter-ELM losses are observed only above a threshold in q_{95}. For EDA-H-mode on Alcator C-mod and pure type-II ELMs on ASDEX Upgrade $q_{95} > 3.5$ is found and for JT-60U the threshold value of q_{95} for pure grassy ELMs is between 4 and 6. In JET, an increase of q_{95} from 3 to 4, or, in a different configuration, from 3.6 to 4.7 led to a significant decrease (20%) of the pedestal density for the same level of gas puff, combined with an increased ELM frequency. Starting from an anchor point at I_p =2.5MA and B_t =2.7T, similar results have been obtained either by raising the magnetic field or by lowering the plasma current. With increased gas puff the density can be recovered, but only at reduced energy confinement and very high frequent ELMs; probably type-III. This means that a regime with $H98(y,2) \approx 1$ and $q_{95} > 4$ has not been achieved at JET with any ELM type at plasma currents above 2MA. There appears to be a significant dependence of particle confinement on q_{95} specifically between ELMs [12], but the reasons for this are still unclear.

3. DIMENSIONLESS IDENTITY WITH SMALL ELM REGIMES ON ALCATOR C-MOD AND ASDEX UPGRADE

A possible way to analyse the failure to obtain pure small ELM phases in JET at plasma currents above 2MA are dimensionless identity experiments at low plasma current matching the respective plasmas in smaller machines. As shown by [17] the dimensionless parameters which govern the dimensionless equations for the fully ionized plasma are ρ^*, ν^*, β, q_{95}, and of course the geometry, i.e. ϵ and the poloidal cross section (explicitely excluding effects on the scale of the Debye length, which would require additional dimensionless parameters).

The constraint that ρ^*, ν^*, β, q_{95} have to be constant leads to a unique size scaling for the dimensional parameters. As a consequence, the smaller machine has to operate at the upper bound of its operational parameters whereas the larger machine (here: JET) has to operate at the lower bound, well below its design values. Since $B_t \cdot \tau_E$ is an invariant of the scaling [18], all frequencies described by the plasma equations are expected to scale with the minor radius α as $f \propto 1/\tau \propto B \propto \alpha^{-1.25}$, using $B \propto \alpha^{-1.25}$ from [17]. For two machines with minor radii α_1, α_2 it follows $f_1/f_2 = (\alpha_2/\alpha_1)^{1.25}$. This holds for example for dimensionless identical ion-cyclotron-resonance-heating (ICRH) and the ratio of the frequencies of dimensionless identical MHD-modes. It should be noted that the scalings can be violated if atomic physics or effects on the scale of the Debye length play an important role. Since the H-mode pedestal region is most affected by ELMs, the above mentioned dimensionless parameters should be matched in this region for comparison of the ELM behaviour.

A source of ambiguity is usually the additional heating since NBI heating clearly involves atomic physics and scaled ICRH frequencies may not be available. Also fueling by wall recycling and gas puff does not happen according to the scaling requirement (i.e. the radial width of the particle-source profile does not scale with the major radius). Earlier pedestal dimensionless identity experiments showed that for example the L/H threshold [19] in JET and ASDEX Upgrade can be well scaled using the same value of ρ^*, ν^*, β, but not between ASDEX Upgrade and Alcator C-mod [20] hindering similar EDA-dimensionless-identity experiments such as those reported below for JET and Alcator C-mod.

3.1. PEDESTAL DIMENSIONLESS IDENTITY TO EDA-H-MODE

The EDA-H-mode in Alcator C-mod is found above certain thresholds in δ, q_{95}, and the pedestal density n_{ped} and shows good H-mode confinement, close to the (non-steadystate) ELM-free H-mode [8]. It is characterized by continuous MHD activity and density fluctuations between 60kHz and 120kHz of rather narrow band width, located in the steep gradient region. These fluctuations are called the quasi-coherent mode (QCM). At higher pedestal temperatures T_{ped}, a transition to a grassy ELM regime is observed and the edge MHD frequency drops and becomes broadband (see for example Fig.4 in [8], where the grassy ELM MHD is observed in the whole frequency range between the original QCM and zero). It should be noted that the term “grassy ELMs” is used on various machines for small ELMs which are neither type-I nor type-III. This does not mean that the grassy ELMs on different machines are necessarily the “same thing”. For example, the grassy ELMs on Alcator C-mod occur in a collisionality range close to the type-II ELMs of ASDEX Upgrade but significantly higher than the grassy ELMs in JT-60U, which are discussed in section 4. Still, in this paper we use the original names given to the specific small ELM regimes in the original publications. After some iterations, a very good shape match between JET and Alcator C-mod was achieved (Fig.3). The reference Alcator C-mod discharge shows the usual EDA behaviour. The experiments are described in detail in [15, 16]. The main difficulty in JET is the diagnosis of the edge pedestal as the JET diagnostic set was not designed to operate in this operational range (I_p = 0.65MA, B_t = 0.9T). Therefore, an uncertainty on the pedestal pressure of about 50% remained, spanning the scaled value from Alcator C-mod, essentially due to uncertainties in the pedestal temperature [16]. Nevertheless, in the steep gradient zone at the plasma edge, good agreement of ∇n_e, ∇T_e with the scaled values of Alcator C-mod was observed. It remains uncertain to what extent dimensionless identical plasmas have been achieved. The error bar of the pedestal temperature in these low-current JET-plasmas even includes the scaled T_{ped}-threshold of Alcator C-mod, which separates EDA and grassy-ELM behaviour. Additionally, the plasma behaviour depends crucially on small variations of the lower triangularity and on the heating method, which was either NBI or 2nd harmonic hydrogen minority heating with ICRH, in contrast to 1st harmonic minority heating at Alcator C-mod (i.e. ICRH frequencies could not be matched according to dimensionless scaling). No controlled EDA modes have been found at JET, but phases with a

steady pedestal were observed for several τ_E (up to 1s). Magnetic and density fluctuation patterns observed with pick-up coils and a reflectometer are variable in terms of strength and bandwidth. Often the fluctuations are enhanced in the 10kHz to 20kHz range. They rotate in the direction of the electron diamagnetic drift as observed for the QCM in Alcator C-mod. The bandwith Δf of these enhanced fluctuations in JET is occasionally lower than 1kHz. In such cases at least two harmonics of a base frequency of 10 to 15kHz are observed (higher ones are very weak) [15, 16]. According to the dimensionless identity scaling, this frequency does correspond to the frequency range of 60 to 90kHz at Alcator C-mod, which is within the frequency range of the quasi coherent mode. Nevertheless, multiple harmonics are never observed with this shape at Alcator C-mod so that the observations on both machines do not exactly match.

In JET these phases without ELMs and with constant n_{ped}, T_{ped} are observed with NBI as well as with ICR heating. With ICRH, fluctuation patterns with a band-width comparable to the QCM have been observed [15, 16]. A pure NBI-heated case is shown in Fig.4, which shows one of the longest phases with steady pedestal conditions. Under these conditions edge density fluctuations are strongest in the upper half of the steep gradient zone, whereas in Alcator C-mod they are found in the lower half. With ICRH as well as with NBI, an increase of radiation leads to a transition to type-III ELMs with poorer confinement. The increase of radiation is observed simultaneously with a central peaking of the density profile. This recalls observations in DIII-D [21], ASDEX Upgrade [22], Alcator C-mod [23], and JET [24], in which a slow central density peaking has been observed for broad or off-axis peaked profiles of auxillary heating. Without further analysis it remains a speculation that similar effects could play a role in this case: As mentioned above, we know that the available auxillary heating schemes violate the dimensionless scaling approach. In H-modes, due to the strong density pedestal, NBI heating (as used in JET) always results in a much broader heating profile than central 1st-harmonic ICR minority heating (as used in Alcator C-mod). Also for the 2nd harmonic ICR minority heating in JET, one may speculate that poorer single pass absorption and possibly additional impurity resonances at the plasma edge do broaden the heating profile. It remains to be verified that these differences in the heating profiles are really the reason for the observed differences in the central density profile evolution.

3.2. DIMENSIONLESS IDENTITY APPROACH FOR TYPE-II ELMS AS IN ASDEX UPGRADE

In [3] three criteria were introduced for the characterization of type-II ELMs in ASDEX Upgrade: good H-mode confinement, quasi continuous heat flux to divertor as measured by the infrared cameras (IR) and broadband fluctuations in density and magnetics in the steep gradient zone of the edge pedestal ranging from 20kHz to 40kHz. Type-II ELMs are observed in QDN configurations with $q_{95} > 3.5 \ldots 4.0$ in a narrow density band just below the transition to type-III ELMs. Steady state phases with pure type-II ELMs are only observed when q_{95} is above a threshold value which varies between 3.5 and 4.0, depending on plasma shape and β. As described in [3], a reduction of

q_{95} below the threshold leads to a mixture with type-I ELMs and the bandwidth of the inter-ELM fluctuations is reduced. Under these conditions the fluctuation occur in quite regular bursts ($\approx$ 0.5 . . . 1kHz). Such a phase has been revisited for the comparisons in this paper. The result is shown in Fig.5 (and as lower curve in the right part of Fig.6, which shows the peaks in the reflectometer spectrum more clearly). The highly localised reflectometer measurement shows two bands around 13 and 25kHz during the mixed I/II phase whereas the MHD is more broadband in between 10 and 30kHz. This MHD structure is sharp enough to determine its mode number, yielding $n \leq 4$ and $m \geq 12$, again in the direction of the electron diamagnetic drift. The MHD fluctuations between 150 and 200kHz had been overlooked earlier, but they are present in all type-II phases published in [3] and disappear at transitions to type-III ELMs. The mode numbers are in this case n=5 . . . 7, $m \geq 12$, electron direction. More recent type-II experiments show that the MHD/reflectometer footprint are not found at higher power and/or strong ICRH (> 3MW) although the other two criteria still hold. As an example Fig.6 shows the magnetic spectrogram and the spectrum of edge-density-fluctuation for an improved H-mode with high β_N and type-II ELMs at q_{95} = 3.5 as described in [4]. This does not necessarily mean that the modes are not present, they may be hidden by the significantly higher amplitude of all frequencies in the analysed frequency range or the radial location of the density fluctuation measurement may have changed slightly due to changes in the density pedestal-profile.

Due to differences in the sets of poloidal-field coils a close shape match of the high-δ ASDEX Upgrade equilibria was impossible at JET, so that a QDN configuration with the same average δ has been chosen as shown in Fig.7. To reduce the diagnostic problems at very low currents discussed in the previous section, the plasma current in JET (I_p = 0.9MA, Bt = 1.2T, q_{95} = 4.1) was chosen to correspond to a 1MA ASDEX Upgrade discharge although only 0.8MA were run at ASDEX Upgrade with the high-δ shape used in [3]. Figure 8 shows that indeed long phases without ELMs and steady pedestal parameters have been achieved. As in the case of the EDA identity (Fig.4) the central density slowly rises, terminated by the loss of sawteeth and a radiation collapse. In the previous section we speculated that this was due to the broader heat deposition pro le in JET as compared to the central ICR heating in Alcator C-mod, in accordance with observations on several tokamaks. This explanation does not hold for the density peaking in the JET discharges dimensionally similar to ASDEX Upgrade, since the profile of the NBI heating power in ASDEX Upgrade is almost at, but in the dimensionless identical JET plasma the heating profile is peaked centrally with the maximum around ρ = 0.2. Since the major mismatches in the dimensionless scaling are the heat-flux profile and the shapes in the vicinity of the upper and lower x-points one may speculate about other possible reasons related to these quantities. The most striking difference of the NBI heating in both machines is that in JET about 80% of the heating goes to the electrons, whereas in ASDEX Upgrade this fraction is approximately 50%. It remains an open question if this difference relates to the different behaviour of the central density. In JET/ASDEX Upgrade case also the mismatch in upper triangularity may be responsible for the behaviour, since it is found on ASDEX Upgrade that higher upper triangularity favours the occurrence of slow density peaking and the mismatch of the shapes is indeed such that the JET plasma has a higher upper triangularity as compared to the

ASDEX Upgrade plasma. Also, the steady profiles in ASDEX Upgrade are only obtained if $q_{95} \geq 3.8$, below this value also in ASDEX Upgrade the slow central density peaking is observed. Such a case is shown in Fig.5 (The pedestal density is constant from 3.5s to 4.2s), indicating that small differences in the discharge parameters can indeed trigger an unstable behaviour of the central density.

In the following, the uctuations observed in JET in the region of the steady H-mode pedestal are discussed. Figure 8 shows the spectrogram of an reflectometer channel in the steep gradient region and the MHD mode number analysis for JET Pulse No: 62430. Two sharp bands are observed with the reflectometer at approximately 8 and 15kHz, rather close to what is expected from the dimensionless identity scaling of the frequencies from ASDEX Upgrade to JET as described in the introduction to section 3 (see Fig.5, scaling factor $(\alpha_{AUG}/\alpha_{JET})^{1.25} \approx 0.5$, using $(\alpha_{AUG}/\alpha_{JET}) = 1.78$ from Fig.7). As in ASDEX Upgrade the MHD fluctuations are less sharp and again they move in the direction of the electron drift. The n-number of the mode between 15 and 20kHz is close to 4, the minimum m-number is estimated to be 7, a lower limit depending on the present set of pick-up coils. These numbers also relate well to the findings on ASDEX Upgrade (n=4, m>12). After 23.7s the bandwidth of the modes measured with the reflectometer increases and the frequency drops in contrast to the MHD analysis. Due to the strong radial localisation of the reflectometer this could be due to the still slightly increasing edge density, shifting the location of the measurement further towards the separatrix and possibly away from the mode. In any case this example shows that bandwidth and frequency of the observation are subject to a signi cant variation. We also note that the upper frequency bands observed in ASDEX Upgrade (see Fig.5) should appear around 100kHz in JET according to the scaling. Fig.9 shows a discharge where the small ELM phase is shorter but with magnetic data at a higher sampling frequency. Indeed, a weak band is observed in the magnetics at 110kHz, rotating in the expected electron drift direction, with $n \approx 2$ which is lower than in ASDEX Upgrade. After having successfully established the scenario at JET using the dimensionless identity approach, the intension was to increase plasma current and magnetic field. The plasma current was increased from 0.9MA to 1.2MA and 1.5MA at fixed q_{95}. Fig 10 shows that for 1.2MA only mixed type-I/II phases were obtained with the type-II phases lasting up to 0.3sec. At 1.5MA only high frequent type-I ELMy H-modes were found (see figure in [12]) resembling the behaviour observed at $q_{95} \approx 4$ at higher plasma currents as mentioned in section 2. Although the search at the higher currents was rather coarse due to time limitations, the failure indicates that it is more difficult if not impossible to get the pure type-II phases with increasing current, especially since the low current scenario was obtained in three campaigns during 2003 in a quite straight forward manner, using a coarse gas scan.

4. THE HIGH β_{pol} GRASSY ELM SCHEME OF JT-60U APPLIED TO JET AND ASDEX UPGRADE

Another small ELM regime with good confinement is the grassy ELM regime observed in JT-60U. The most recent publication is [6]. As reported by JT-60U [5] a high value of β_{pol} facilitates operation with grassy ELMs most probably due to the stabilising effect of a strong Shafranov-shift [25, 26].

The regime is observed as β_{pol} exceeds a value of 1.4 . . . 2.0 depending on q_{95} and δ. High values of the latter two quantities favour the occurrence of the grassy ELM regime. Typical values are $\beta_{pol} \geq 1.6$ and $q_{95} \approx 6$ for $\delta \approx 0.5$. The grassy ELM regime can be extended toward lower q_{95} ($q_{95} < 4$), by increasing the triangularity up to $\delta \approx 0.6$ [25]. Usually the regime is operated with an internal transport barrier using early heating to avoid the occurrence of sawteeth. Figure 11 shows the time-traces of JT-60U Pulse No: 42857, which has been used to compare the magnetic uctuation signals to those obtained at JET, as discussed below. The grassy ELM regime has significantly lower collisionality $\nu^*_{ee} \approx 0.1$ as compared to the high density small ELM regimes discussed above which have $2 \geq \nu^*_{ee} \geq 0.5$. This triggered experiments to transfer it to JET and ASDEX Upgrade. These experiments were not meant to match the JT-60U plasmas in the strict sense of a dimensionless identity experiment, but the key ingredients high β_{pol}, high δ and high q_{95} have been used for plasmas that showed already signs of mixed type-I/II ELMs at lower values of q_{95} and β_{pol}.

4.1. HIGH β_{pol} GRASSY ELM EXPERIMENTS AT JET

In JET, the shape developed for the identity experiment with ASDEX Upgrade was also used for the high β_{pol} experiment, with somewhat increased plasma current (1.2 . . . 1.5MA), but strongly increased magnetic field (2.7T) and plasma heating (17MW to 23MW, i.e. all power available on the day). This also means that the configuration was close to DN. Above a β_{pol} - value of 1.8 only very small ELMs are observed [12]. The energy carried by them is so small that it cannot be quantified (<5% of W_{ped}) in contrast to the type-I ELMs at lower β_{pol} which each carry 15% or more of W_{ped}. The magnetic spectrogram and the fast D_α trace of such a JET-grassy-ELM phase are shown in Fig.12. They are compared to a grassy ELM phase of JT-60U Pulse No: 42857 (Fig.11). The spectrograms look similar. In particular there are no modes seen in the range of a few 10kHz or at even higher frequencies. Such high values of β_{pol} could only be achieved at JET at $I_p = 1.2$MA due to limitations in heating power. There is no evidence that this is a physics based limit. In parallel to these experiments another set of high β_{pol} discharges has been run at JET to study the effect of the high β_{pol} on the core transport together with a flat q- profile and consequently lower l_i and higher edge currents, using Lower Hybrid pre-heating and early main heating. Further differences are that the plasma shape was clearly a lower SN shape and that the pedestal collisionality was about 50% lower. Interestingly no grassy ELMs were observed even at $\beta_{pol} = 1.9$ [12]. Obviously the relative importance of the above mentioned differences has to be separated by further experiments.

4.2. HIGH β_{pol} GRASSY ELM EXPERIMENTS AT ASDEX UPGRADE

The high β_{pol} strategy has also been tried recently on ASDEX Upgrade. Pure grassy ELMs were found with a configuration close to DN [27]. The plasma shape is close to the original type-II shape [3], with stronger heating (14MW) similar to the improved H-modes which can be integrated with type-II ELMs [4]. In contrast to these earlier experiments q_{95} is increased to ≈ 7 to access the grassy ELM regime according to the operational boundaries determined at JT-60U. This is done by increasing B_t to 3T keeping I_p =0.8MA. The resulting grassy ELM regime could indeed be accessed

at lower densities as compared to the original type-II regime. ν^* is more than a factor 3 smaller than in the original type-II regime and similar to the value of 0.6 obtained in the above mentioned improved H-modes with small ELMs at lower q_{95}. The spectrogram of a magnetic pick-up probe is shown in the central part of Fig.13. It is similar to what has been found on JT-60U and JET (Fig.12), although the affected frequency region extends up to 10kHz, perhaps due to the smaller machine size. For a very similar SN configuration only mixed type-I/grassy phases were obtained. In this case the magnetic fluctuations occur in the same frequency range, but are correlated in time with the remaining type-I ELMs (vertical bars in upper part of Fig.13). Infrared divertor thermography shows high bursty H_α-correlated heat ux on the outer plate only for the SN case whereas for the DN case the heat ux remains steady at the inter-ELM level of the SN case. It is not clear in how far these high-q_{95} grassy ELMs are different from the earlier type-II ELMs, in as much as there are differences in the MHD spectra. As already mentioned, type-II ELMs are also found in improved H-modes [4]. These plasmas have $q_{95} = 3.5$ lower than the earlier type-II plasmas but a $\beta_{pol} \approx 1.6$ close to that of the grassy ELMs at high q_{95}. As shown in Fig.6, they do not show enhanced fluctuations below 5kHz nor the modes at a few 10kHz. The edge density uctuation spectra for the high q_{95}-case grassy ELMs (Fig.13 bottom) and the low q_{95}-case so far identified as type-II ELMs (Fig.6 right) are very similar and it remains to be verified if there is a continuous transition between both and at which value of q_{95} the magnetic fluctuations at a few kHz set in.

CONCLUSIONS

H-modes with an edge behaviour reminiscent of EDA, high density type-II ELMs and high β_{pol} grassy ELMs have been developed at JET, of which only the latter was fully controlled, whereas the others were limited by radiation collapses due to central density peaking. The operational regime is restricted to plasma currents below 1MAfor the pure type-II ELMs. The mixed type-I/II phases observed at JET earlier at 2.5MA, could also not be transferred to pure type-II phases by using quasi-DN configurations nor higher values of q_{95}. In dimensionless parameters, essentially ρ^* and ν^* decrease with increasing current. Although the change in ρ^* is larger, the change in ν^* is usually favoured as an explanation for this current scaling, since it directly influences the edge bootstrap current and therefore the stability of edge current driven peeling modes [28, 29]. The plasmas which were meant to be dimensionlessly identical to either the EDA mode in Alcator C-mod or to the type-II ELMs of ASDEX Upgrade were very similar in terms of mode activity observed in the magnetic and reflectometer signals in JET, indicating a close relation between both phenomena. Nevertheless it must be noted that only part of this turbulence footprint matches the observations on Alcator C-mod and ASDEX Upgrade. A striking difference between both sets of experiments is that the EDA experiments were done in the same SN configuration which shows the mixed type-I/ II ELMs at higher current whereas the type-II identity shots were done in a QDN configuration which is a prerequisit for pure type-II ELMs in ASDEX Upgrade. An explanation for these contradictory findings could be that rather a quantity related to QDN, for example the magnetic shear in the steep gradient region is a crucial parameter. In the specific JET SN configuration it may

be created by other moments of the shape. As mentioned above, also the high β_{pol} plasmas in JET only showed pure grassy ELMs when close to DN, but other parameters, especially the current-density at the plasma edge, were changed as well. These effects can only be separated in future experiments.

In JET, for the high β_{pol} scheme, the current was limited to 1.2MA, but this is due to a limit in additional heating power. The high β_{pol} discharges on JET and ASDEX Upgrade showed similar uctuations in the MHD spectrogram as observed in JT-60U. Nevertheless, they were at least a factor 4 higher in ν^* than those observed in JT-60U ($\nu^*_{JT\text{-}60U} \approx 0.1$), whereas in JET the low l_i discharges with high β_{pol} reached approximately the JT-60U collisionality values but did not show grassy ELMs. This is especially striking since the JT-60U discharges are usually also operated with early heating. An experimental separation of the relevance of ν^*, l_i, q_{95} and closeness to DN for the appearance of grassy ELMs at high β_{pol} in JET is still outstanding.

In view of a future reactor plasma, our results suggest that only the high β_{pol} scheme may be extrapolatable, but means have to be found to run it at lower values of q_{95}, as was possible on JT-60U using very strong shaping ($\delta \approx 0.6$) [25].

REFERENCES

[1]. Loarte, A. et al., Phys. Plasmas **11** (2004) 2668.

[2]. ITER Physics Basis, Nucl. Fusion **39** (1999) 2137, for confinement scaling IPB98(y,2) see page 2204.

[3]. Stober, J. et al., Nucl. Fusion **41** (2001) 1123.

[4]. Sips, A.C.C. et al., Plasma Phys. Controlled Fusion 44 (2002) A151.

[5]. Kamada, Y. et al., Plasma Phys. Controlled Fusion 42 (2000) A247.

[6]. Oyama, N. et al., Nucl. Fusion , submitted.

[7]. Greenwald, M. et al., Phys. Plasmas **6** (1999) 1943.

[8]. Mossessian, D.A. et al., Plasma Phys. **10** (2003) 1720.

[9]. Suttrop, W. et al., in *Proc. of the 20th IAEA Conference Fusion Energy, Vilamoura, Portugal, November 2004*, volume IAEA-CSP-25/CD, pages CD-ROM le EX/1-4 and http://www-naweb.iaea.org/napc/physics/fec/fec2004/datasets/index.html, Vienna, 2005, IAEA.

[10]. Saibene, G. et al., Plasma Phys. Controlled Fusion **44** (2002) 1769.

[11]. Sartori, R. et al., in *Proc. of the 20th IAEA Conference Fusion Energy, Vilamoura, Portugal, November 2004*, volume IAEA-CSP-25/CD, pages CD-ROM le EX/6-3 and http://www-naweb.iaea.org/napc/physics/fec/fec2004/datasets/index.html, Vienna, 2005, IAEA.

[12]. Saibene, G. et al., Nucl. Fusion **45** (2005) 297.

[13]. Perez, C.P. et al., Plasma Phys. Controlled Fusion **46** (2004) 61.

[14]. Smeulders, P. et al., Plasma Phys. Controlled Fusion **41** (1999) 1303.

[15]. Maddison, G.P. et al., EDA H-mode pedestal identity studies on JET and Alcator C-Mod, in Europhysics Conference Abstracts (CD-ROM, Proc. of the 30th EPS Conference on Controlled

Fusion *and Plasma Physics, St. Petersburg, 2003)*, edited by Koch, R. and LEBEDEV, S., volume 27A, pages P-1.109, Geneva, 2003, EPS.

[16]. Mossessian, D.A. et al., H-mode pedestal physics studies in local dimensionless identity experiments, in Europhysics Conference Abstracts (CD-ROM, Proc. of the 30th EPS Conference on Controlled Fusion *and Plasma Physics, St. Petersburg, 2003)*, edited by Koch, R. and Lebedev, S., volume 27A, pages P-3.182, Geneva, 2003, EPS.

[17]. Kadomtsev, B.B., Sov. J. Plasma Phys. **1** (1975) 295.

[18]. Connor, J.W. and Taylor, J.B., Nucl. Fusion **17** (1977) 1047.

[19]. Suttrop, W. et al., Fusion Science and Technology **44** (2003) 636.

[20]. Suttrop W.A. et al., Parameter similarity studies in JET, ASDEX Upgrade and ALCATOR C-Mod, in *Proc. of the 19th IAEA Conference Fusion Energy (CD-Rom), Lyon, France, October 2002*, volume IAEA-CSP-19/CD, pages CD-ROM le EX/P5-07 and http://www.iaea.org/programmes/ripc/physics/fec2002/html/fec2002.htm, Vienna, 2003, IAEA.

[21]. Mahdavi, M.A. et al., Nucl. Fusion **42** (2002) 52.

[22]. Stober, J. et al., Nucl. Fusion **43** (2003) 1265.

[23]. Rice, J.E. et al., Nucl. Fusion **43** (2003) 781.

[24]. Valovic, M. et al., Plasma Phys. Controlled Fusion **44** (2002) 1911.

[25]. Kamada, Y. et al., Plasma Phys. Controlled Fusion **44** (2002) A279.

[26]. Saarelma, S. and GÄ UNTER, S., Plasma Phys. Controlled Fusion **46** (2004) 1259.

[27]. Horton, L.D. et al., Max-Planck-Institut f¨ur Plasmaphysik, Garching, Germany, private communication.

[28]. Saarelma, S. et al., Nucl. Fusion **43** (2003) 262.

[29]. Lönnroth, J.-S. et al., Plasma Phys. Controlled Fusion **46** (2004) 767.

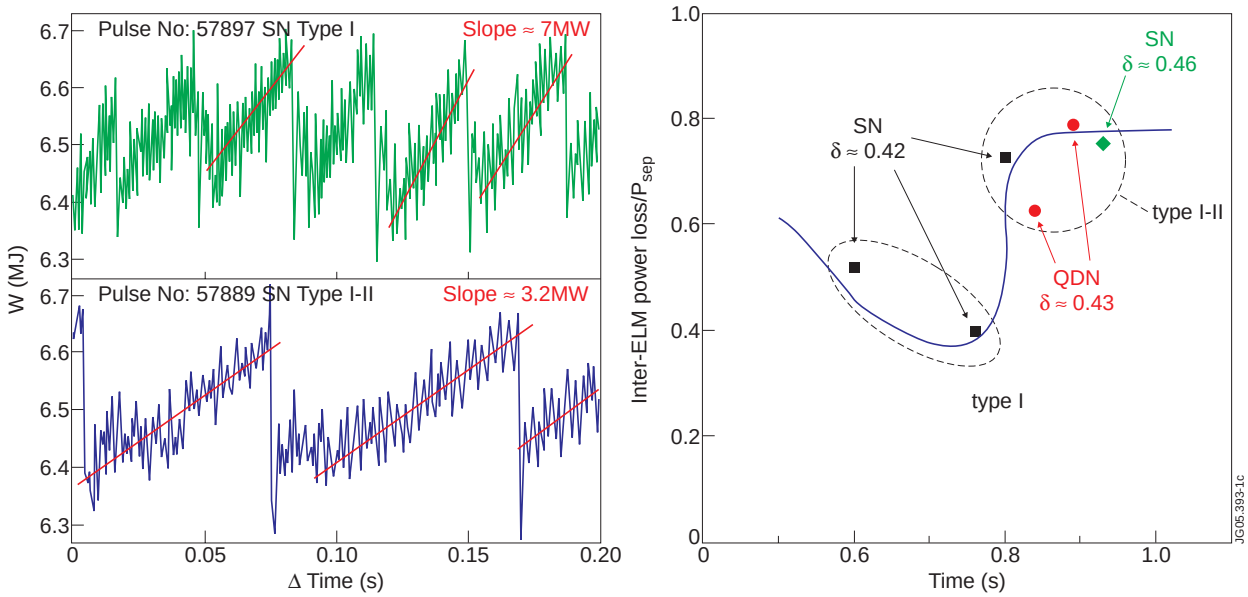

Figure 1: Mixed type-I/II H-modes in JET, I_p = 2.5MA. Left: Time evolution of the stored energy for two discharges with the most frequently used HT3-configuration (q_{95} = 3.5). The discharges have similar control parameters except gas puff. Pure type-I ELMs are observed with moderate gas puff (top, $n_{ped}/n_{GW} \approx 0.6$), mixed type-I/II ELMs are observed with strong gas puff (bottom, $n_{ped}/n_{GW} \approx 0.8$). The difference of the slopes of the inter-ELM energy-rise indicates a change in the inter-ELM energy con nement, i.e. increased inter-ELM losses during mixed type-I/II phases. Right: Inter-ELM contribution to the average power ux across the separatrix (P_{heat} - $P_{rad,\ bulk}$). The blue curve sketches the behaviour for the HT3-configuration (q_{95} = 3.5, black squares), to compare to the behaviour of other configurations (ìITER-likeî: green, QDN: red, both q_{95} = 3.0).

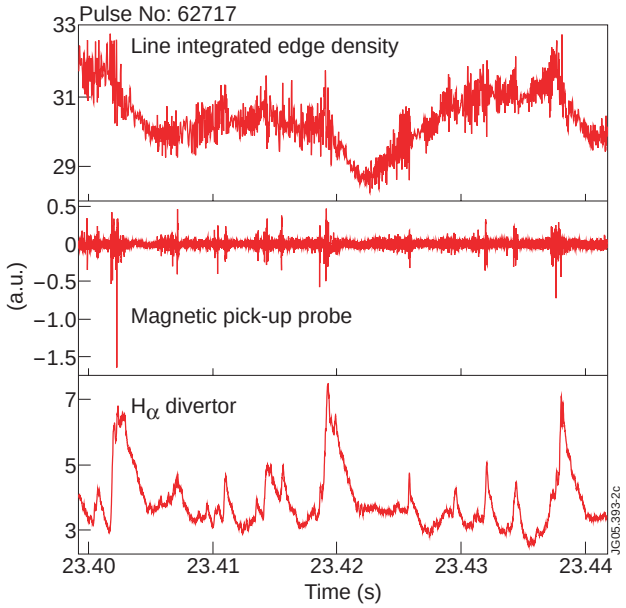

Figure 2: JET Pulse No: 62717, high delta configuration (HT3) at 1.1MA, 1.2T, q_{95} = 3.5. Bottom: divertor H_a showing small bursts between type-I ELMs, which all show up in a magnetic signal from the outer midplane (middle). Top: line integrated edge density from a vertical interferometer channel tangential just inside the H-mode pedestal at the outer midplane. About half of the small bursts present in the lower time traces correlate with a drop of edge density.

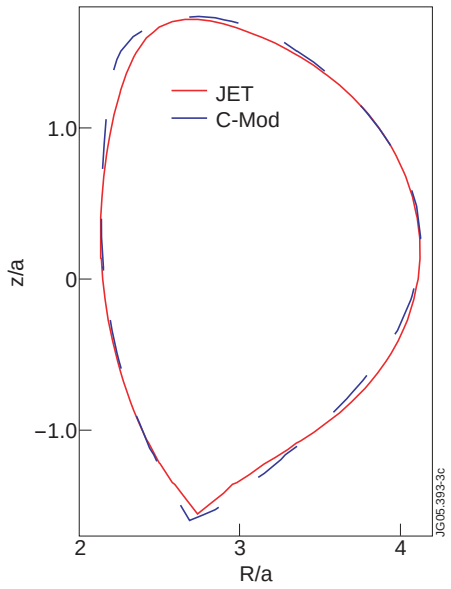

Figure 3: Scaled shapes used for the JET/Alcator C-mod pedestal identity experiments. The JET shape is very close to the HT3 high delta shape, used for the experiments at higher current as described in section 2.

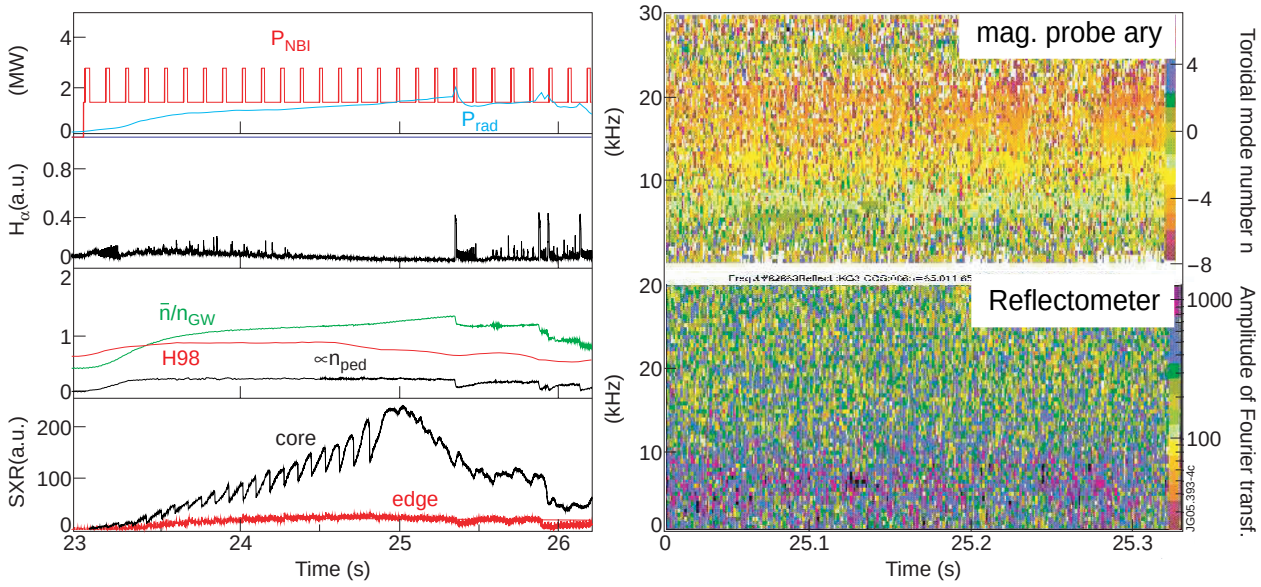

Figure 4: JET pulse 62663, I_p =0.68MA, B_t = 0.94T, q_{95} = 4.2, aimed to be dimensionless identical to Alcator C-mod plasmas. The figures to the right show the toroidal mode number analysis (negative numbers correspond to the electron diamagnetic drift direcrion) and density fluctuations measured in the steep gradient region with the reflectometer (34GHz ≅ 1.4×10^{19} m^{-3})

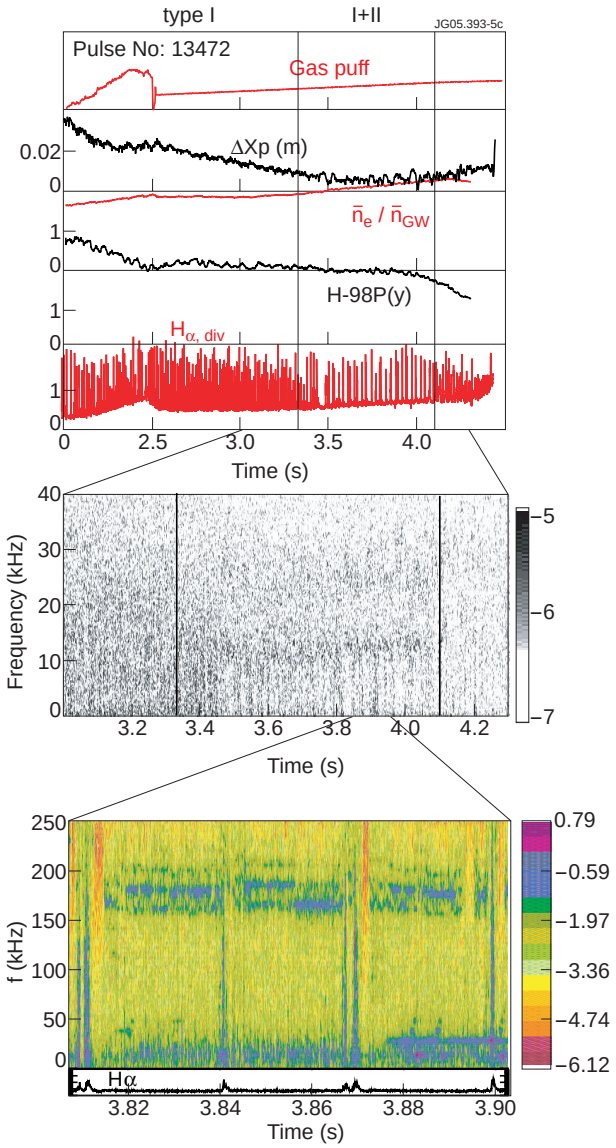

Figure 5: ASDEX Upgrade pulse 13472 0.8MA, 2.0T, q_{95}, (see also [3]), corresponding to a mixed type-I/II phase. (ΔX_p quantities the closeness to a DN configuration. It denotes the distance of the inner separatrix with the lower x-point to the outer separatrix with the upper x-point measured at the outer midplane.) Middle: density fluctuation as seen by a re ectometer channel in the steep gradient region close to the pedestal top. Bottom: spectrogram of a magnetic signal together with an H_α trace from the outer divertor.

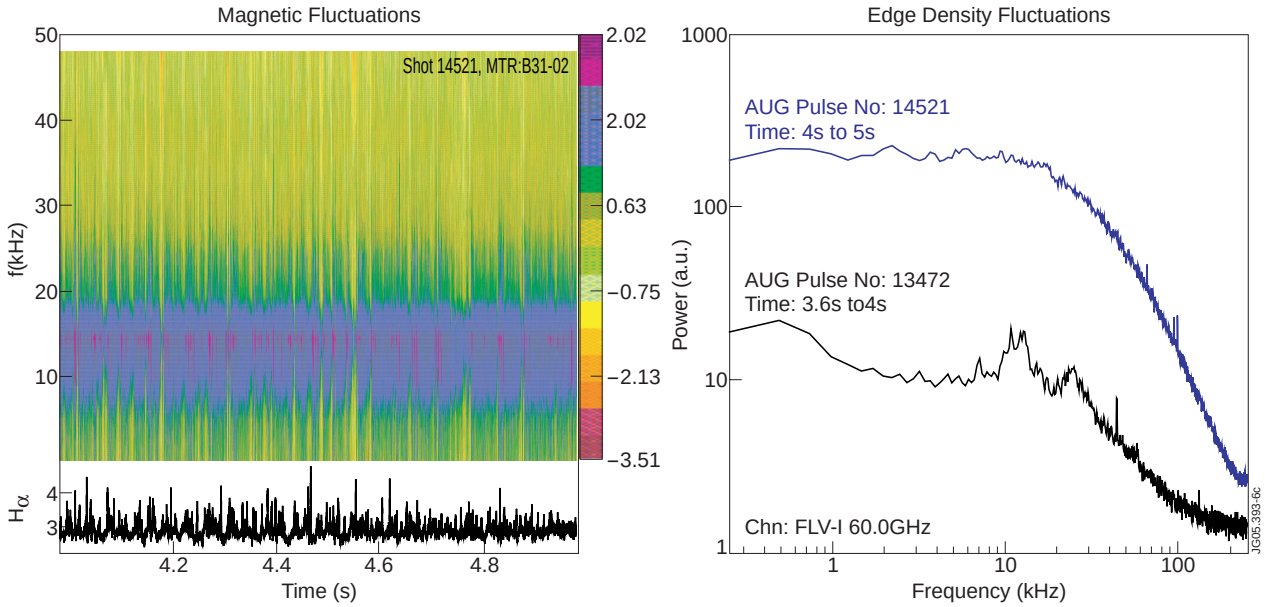

Figure 6: Fluctuation data for ASDEX Upgrade Pulse No: 14521 0.8MA, 1.7T, q_{95} = 3.5, (see also [4]). Compared to Fig.5 the discharge has twice as much heating power, 20% less density, same H-factor and therefore significantly higher temperatures and $\beta_{pol}(\approx 1.7)$ as well as significantly lower pedestal collisionality ($\nu^{*}_{ped} \approx 0.6$). The strong MHD between 8kHz and 18kHz is due to central fishbone and (1,1)-activity. Apart from this frequency range, no enhanced frequency band is observed. Also the reflectometer does not show any frequency bands with enhanced fluctuations in contrast to Pulse No: 13472 from Fig.5. For better comparison also the spectrum of the edge density fluctuations of Pulse No: 13472 is shown. The location of the reflectometer measurement is not exactly the same, since Pulse No: 13472 has a pedestal density which is about 20% higher than Pulse No: 14521. Still, both measurements are located in the upper half of the steep gradient zone. For Pulse No: 14521 the location is closer to the pedestal top.

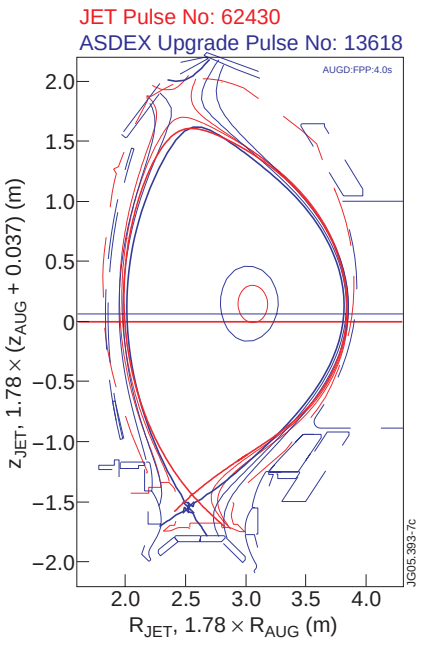

Figure 7: Scaled shapes used for the JET / ASDEX Upgrade type-II identity experiments. Some discrepancies could not be avoided, especially in the outer lower region and the inner upper region. Aspect ratio, elongation and average delta are well matched. The JET equilibrium is a prediction using the PROTEUS code, with the actual coil currents and plasma beta. The ASDEX Upgrade equilibrium is reconstructed from the magnetic data using function parameterisation.

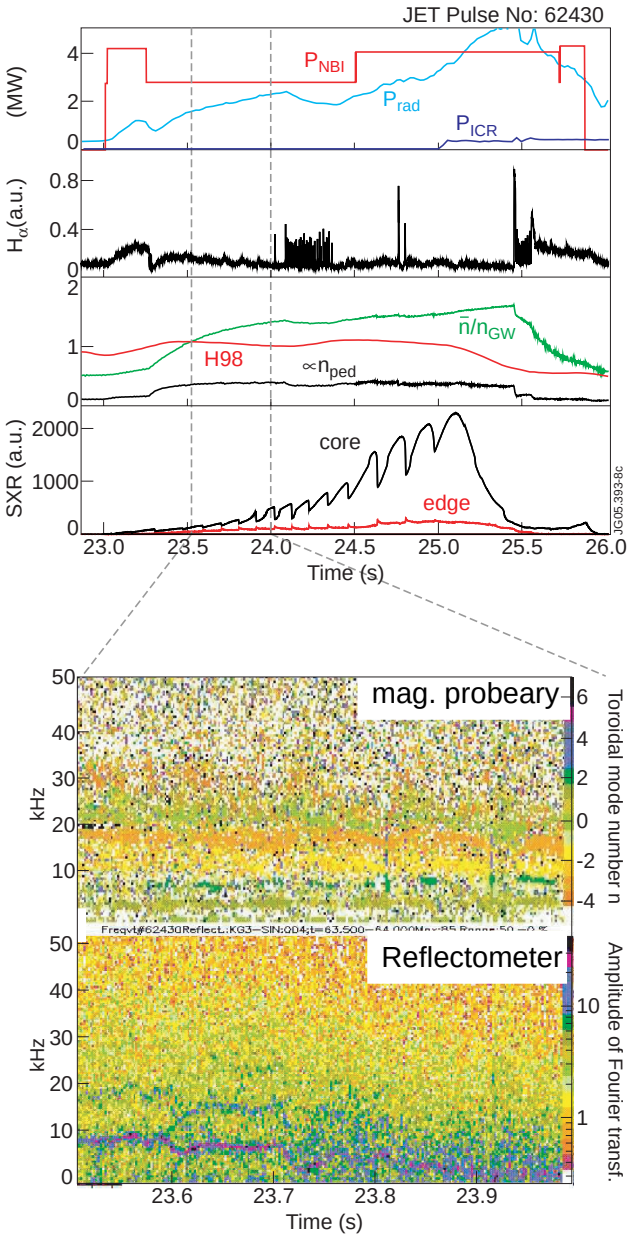

Figure 8: JET Pulse No: 62430, I_p =0.86MA, B_t =1.15T, q_{95}= 4.1, aimed to be dimensionlessly identical to ASDEX Upgrade type-II H-modes. The gures at the bottom show the toroidal mode number analysis (negative numbers correspond to the electron diamagnetic drift direction) and density uctuations measured in the steep gradient region with the reflectometer (34GHz $\cong 1.4 \times 10^{19}\ m^{-3}$)

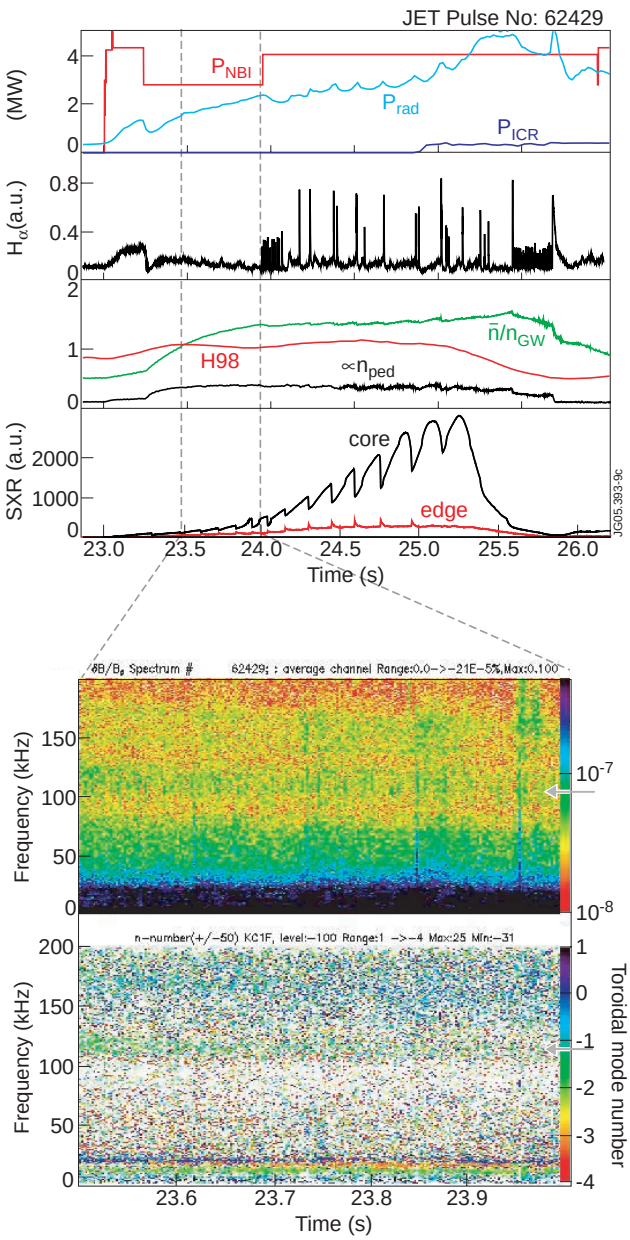

Figure 9: JET Pulse No: 62429, I_p = 0.86MA, B_t =1.15T, q_{95} = 4.1, similar conditions as Fig.8, but faster magnetics available. The gures to the right bottom show spectrogram and toroidal mode number analysis (negative numbers correspond to the electron diamagnetic drift direction) of magnetic data.

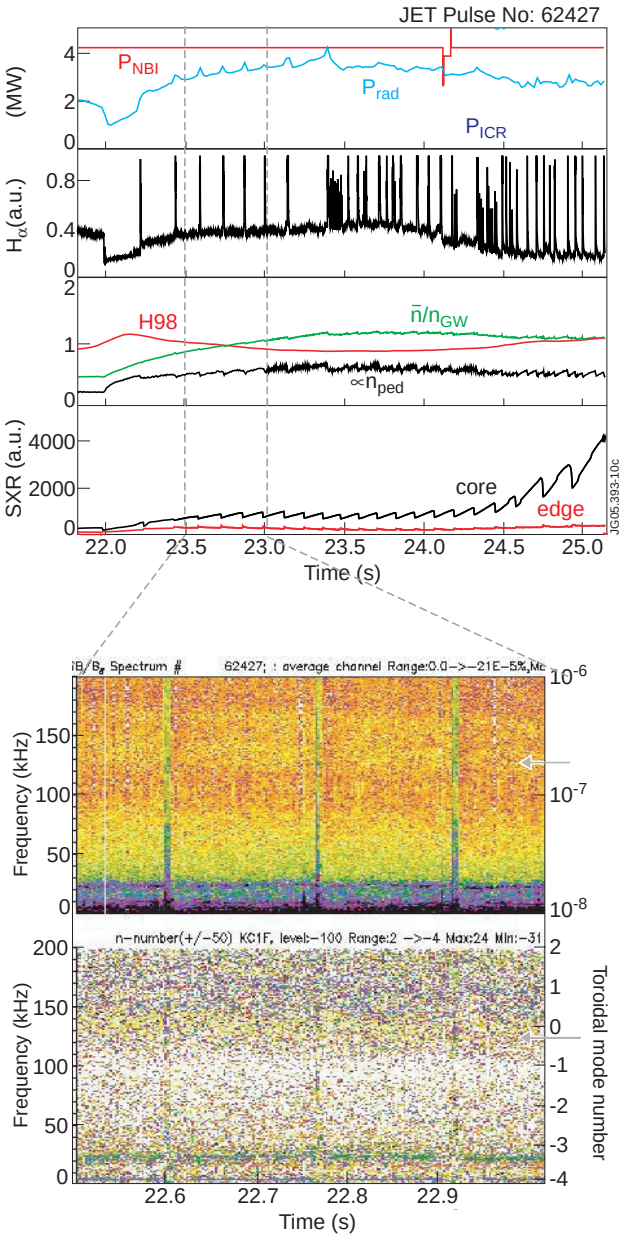

Figure 10: JET Pulse No: 62427, I_p =1.2MA, B_t =1.6T, q_{95} =4.1. The gures to the right bottom show spectrogram and toroidal mode number analysis (negative numbers correspond to the electron diamagnetic drift direction) of magnetic data. In this discharge the gas puff constant up to 23.5s and then ramped down linearly to zero (24.0s).

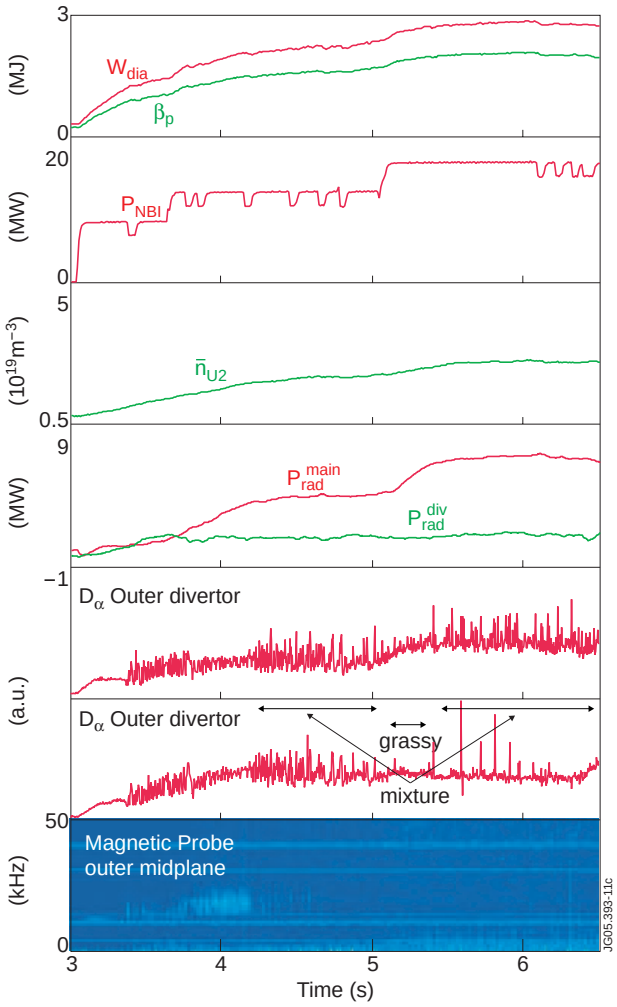

Figure 11: JT-60U pulse E42857, I_p =1.0MA, B_t = 3.6T, q_{95} = 6.4, β_{pol} = 2.0, has pure grassy ELM phase between 5.1 and 5.4s.

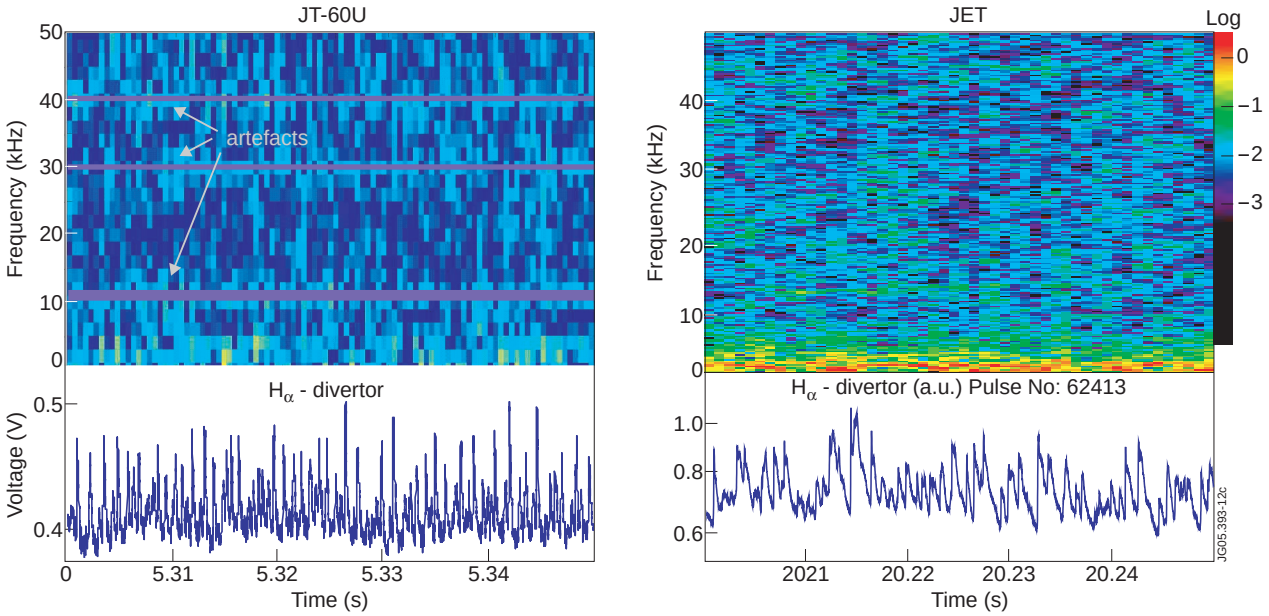

Figure 12: Magnetic spectrograms during grassy ELM phases. JT-60U pulse E42857: I_p =1.0MA, B_t =3.6T, q_{95} = 6.4, $P_{aux} \approx$ 20MW, β_{pol} = 2.0, JET Pulse No: 62413: I_p =1.2MA, B_t =2.7T, q_{95} = 6.9, $P_{aux} \approx$ 23MW, β_{pol} = 1.8.

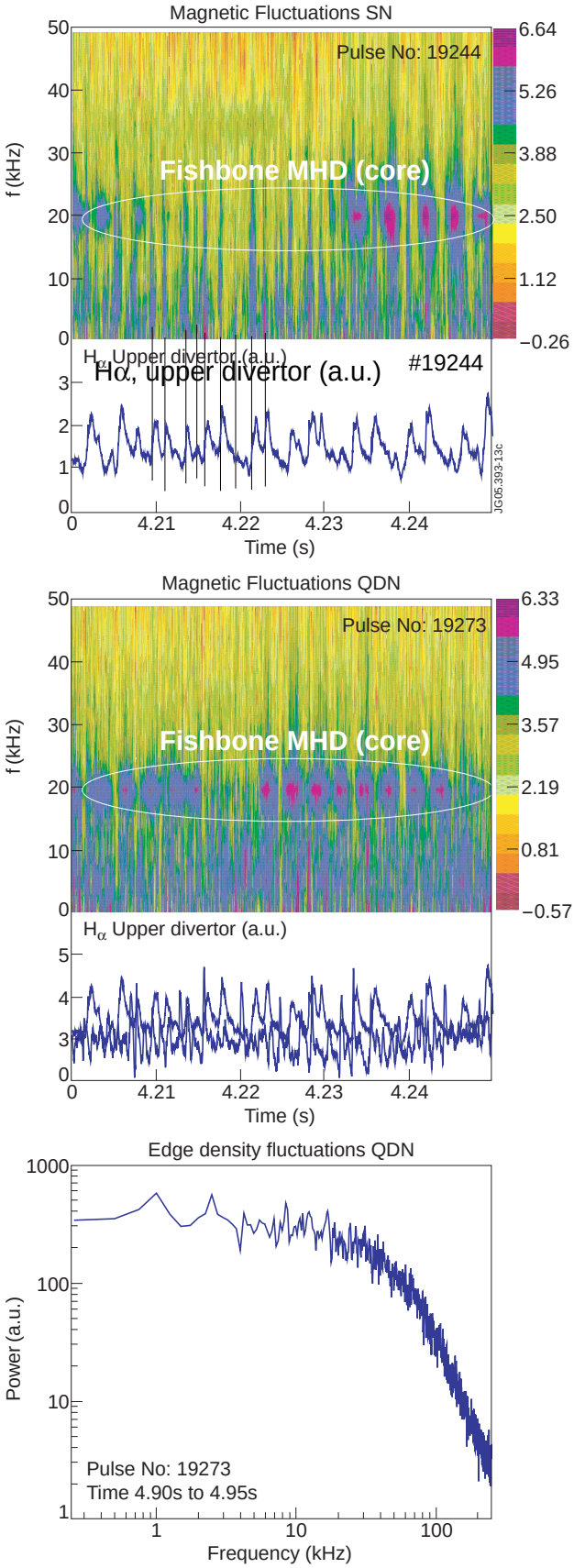

Figure 13: Magnetic spectrograms and H_α traces for two ASDEX Upgrade pulses differing only by the closeness of the second (upper) x-point to the separatrix, i.e. lower SN (Pulse No: 19244, top) and QDN (Pulse No: 19273, middle): I_p =0.8MA, B_t =3T, $q_{95} \approx 6.2$, $P_{aux} \approx 18$ MW, β_{pol} =1.8. At the bottom the spectrum of the density fluctuations is shown for the QDN case, as obtained from reflectometer data from the upper half of the steep gradient zone.